Electronic Supplementary Material

Simultaneous removal of total oxidizable carbon, phosphate and various metallic ions from H_2O_2 solution with amino-functionalized zirconia as adsorbents

Yitong Wang[1], Yue Zhang[1], Li Wang **(✉)**[1,2]

1 School of Chemical Engineering and Technology, Tianjin University, Tianjin 300072, China

2 Zhejiang Institute of Tianjin University, Ningbo 315201, China

E-mail: wlytj@tju.edu.cn

Table S1 Content of metallic ions in hydrogen peroxide solution before adsorption

Metal ions	Contents/(μg·L^{-1})	Metal ions	Contents/(μg·L^{-1})
Li	8.4	Sr	22.33
Be	0.009	Y	0.01
B	3.825	Zr	1.868
Na	2705.110	Mo	2.113
Mg	258.067	Ru	0
Al	1115.766	Ag	0
K	1402.310	Cd	0
Ca	1084.842	Sn	18.645
Ti	16.486	Sb	0.218
V	0.133	Te	0.127
Cr	10.837	Cs	0.898
Mn	2.224	Ba	26.731
Fe	75.24	Ce	6.308
Co	0.071	Nd	0.01
Ni	0	Sm	0.002
Cu	0.82	Pt	0.37
Zn	57.091	TI	0.002
Ga	0.185	Pb	0.021
As	0.288	Th	0.007
Se	0.21	U	0.025
Rb	2.144	Sum	6823.743

Table S2 Content of TOC and acid anions in hydrogen peroxide solution before adsorption

Impurity	Contents/(mg·L^{-1})
PO_4^{3-}	142.660
Cl^-	2.624
SO_4^{2-}	1.271
NO_3^-	0.361
TOC	83.469

Table S3 Content of impurity in hydrogen peroxide solution after adsorption

Adsorbents	TOC /(mg·L^{-1})	PO_4^{3-}/(mg·L^{-1})	Al^{3+} /(μg·L^{-1})	Fe^{3+} /(μg·L^{-1})	Ca^{2+} /(μg·L^{-1})	Mg^{2+} /(μg·L^{-1})
ZrO_2-UN	82.0	115.6	371.4	37.1	753.5	164.2
Zr-N-0.5	27.5	104.8	325.2	32.7	663.8	141.3
Zr-N-1	18.2	98.2	235.2	18.2	563.9	103.2
Zr-N-2	14.5	93.9	187.6	9.7	486.7	86.2

Table S4 Fitting parameters of adsorption kinetic model

Samples	pseudo-first-order model			pseudo-second-order model		
	q_e /(mg·g^{-1})	k_1 /min^{-1}	R^2	q_e /(mg·g^{-1})	$k_2\times10^3$ /(g·mg^{-1}·min^{-1})	R^2
ZrO_2-UN	131.66	0.234	0.9875	142.05	2.497	0.9996
Zr-N-0.5	143.78	0.149	0.9981	152.67	1.788	0.9996
Zr-N-1	159.67	0.180	0.9988	166.11	2.464	0.9997
Zr-N-2	170.51	0.186	0.9986	177.31	2.439	0.9997

Table S5 Fitting parameters of adsorption isotherm model

Sample	Langmuir model			Freundlich model		
	K_L/(L·mg^{-1})	q_{max} /(mg·g^{-1})	R^2	K_F	n	R^2
ZrO_2-UN	0.024	162.5	0.9881	30.48	3.670	0.9164
Zr-N-0.5	0.075	160.8	0.9684	63.87	6.341	0.7935
Zr-N-1	0.080	177.0	0.9515	69.38	6.192	0.7671
Zr-N-2	0.136	186.7	0.9407	85.70	7.250	0.7343

Table S6 Comparison of Zr-N-2 with other zirconium-based adsorbents for adsorption of phosphate

Adsorbents	q_{max}/(mg·g^{-1}) [a)]	Kinetics model	Isotherm model	References
ZrO_2	67.3	PSOM [b)]	Langmuir	[1]
am-ZrO_2	99.0	PSOM	Langmuir	[2]
ZrO_2-a	105.9	PSOM	Langmuir	[3]
HZO	51.8	PSOM	Langmuir	[4]
LBR-Zr	-	PSOM	Freundlich	[5]
ZAE	-	PSOM	Freundlich	[6]
AL-DETA@Zr	167.7	PSOM	Langmuir	[7]
Zr-N-2	186.7	PSOM	Langmuir	This work

a) Maximal adsorption capacity obtained from the fitting of Langmuir model.

b) PSOM: Pseudo-second-order model.

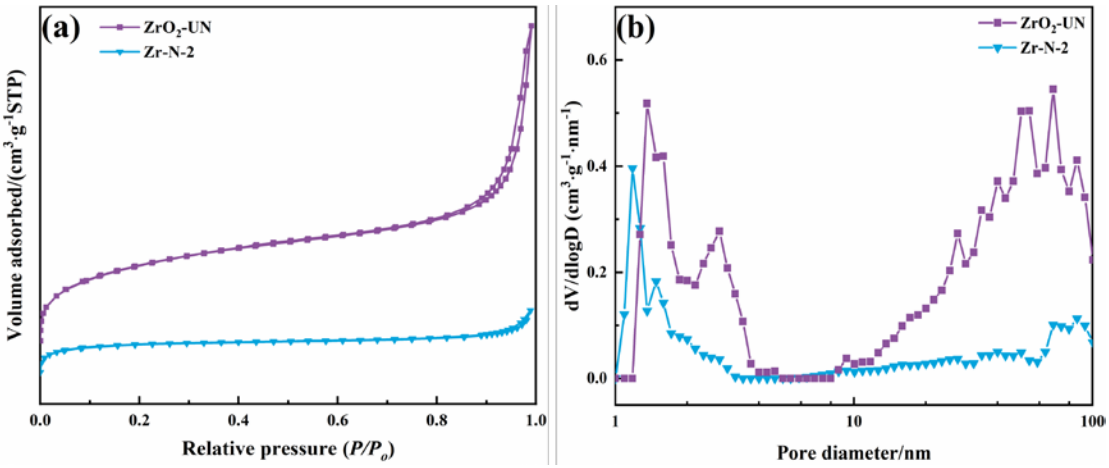

Fig. S1 (a) Nitrogen adsorption-desorption isotherms; (b) DFT pore size distributions of ZrO_2-UN and Zr-N-2.

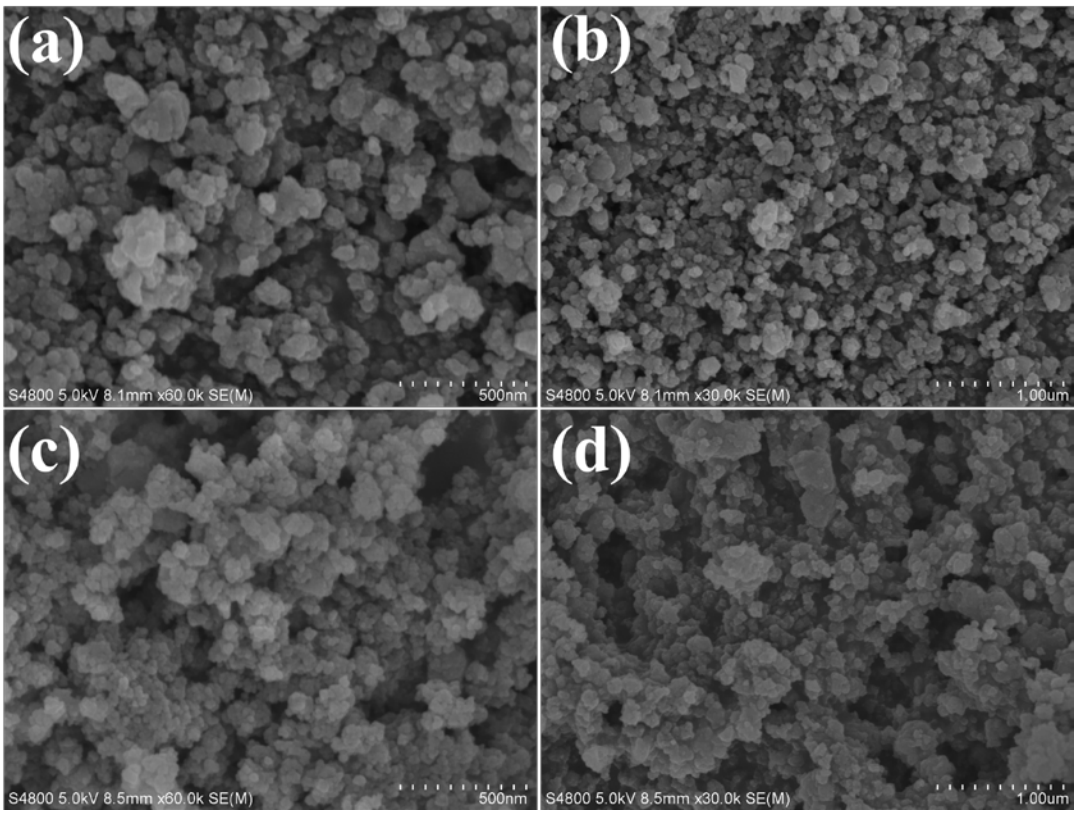

Fig. S2 SEM images of (a) and (b) ZrO_2-UN; (c) and (d) Zr-N-2.

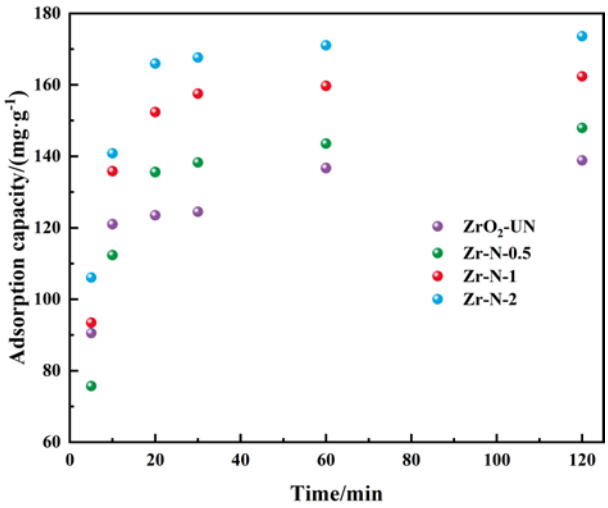

Fig. S3 Effects of contract time on the adsorption of phosphate (Conditions: adsorbent dosage of 1 g/L, pH of 3, initial concentration of 200 mg/L and temperature of 30 °C).

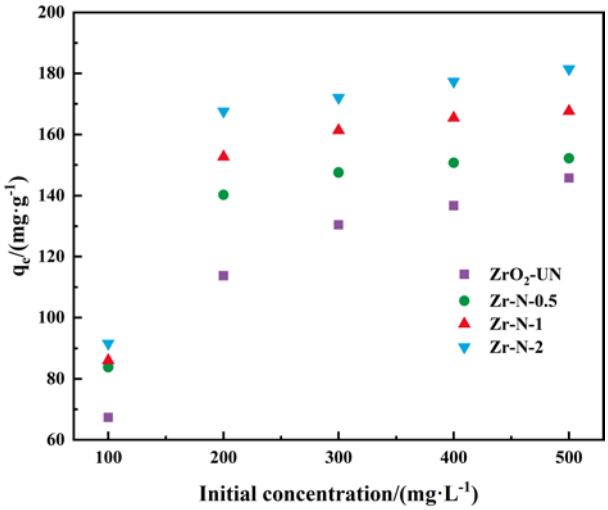

Fig. S4 Effects of initial concentration on the adsorption of phosphate (Conditions: adsorbent dosage of 1 g/L, pH of 3, time of 1 h and temperature of 30 °C).

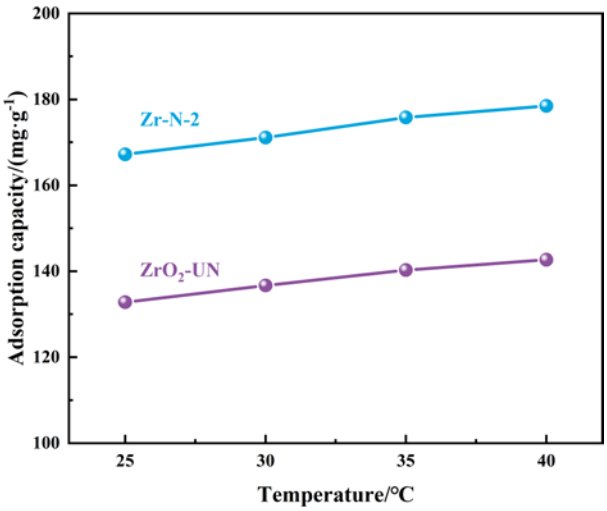

Fig. S5 Effects of temperature on the adsorption of phosphate (Conditions: adsorbent dosage of 1 g/L, pH of 3, time of 1 h and initial concentration of 200 mg/L).

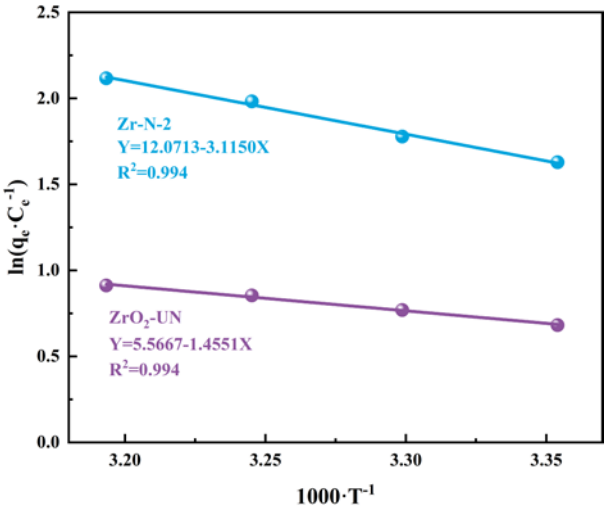

Fig. S6 Thermodynamic data fitting of phosphate in simulated solutions at pH 3 and initial concentration of 200 mg/L.

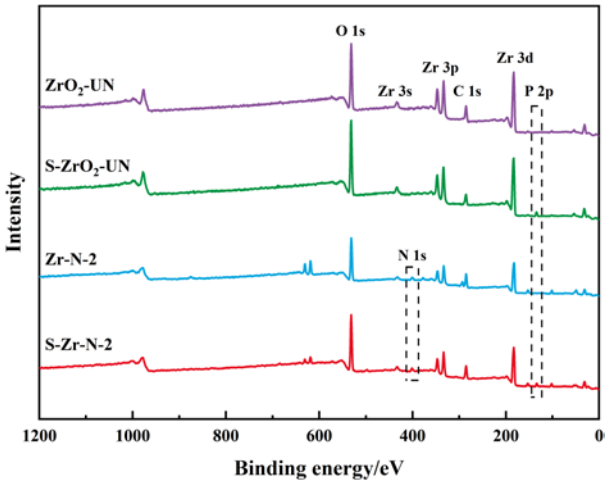

Fig. S7 XPS survey spectra of ZrO_2-UN, S-ZrO_2-UN, Zr-N-2 and S-Zr-N-2.

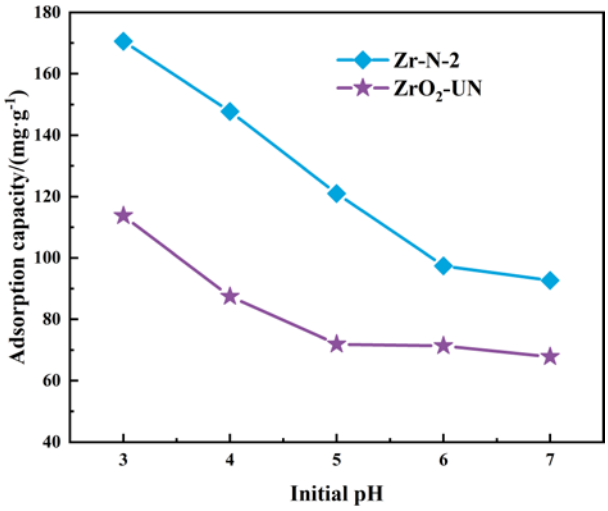

Fig. S8 Effects of initial pH on the adsorption capacity of phosphate (Conditions: phosphate concentration of 200 mg/L, temperature of 30 °C and time of 1 h).

References

1. Lin J, Wang X, Zhan Y. Effect of precipitation pH and coexisting magnesium ion on phosphate adsorption onto hydrous zirconium oxide. Journal of Environmental Sciences, 2019, 76: 167-187

2. Su Y, Cui H, Li Q, Gao S, Shang J. Strong adsorption of phosphate by amorphous zirconium oxide nanoparticles. Water Research, 2013, 47(14): 5018-5026

3. Song L, Li J, Zong H, Lin Y, Ding H, Huang L, Zhang P, Lai X, Liu G, Fan Y. Zirconia

nano-powders with controllable polymorphs synthesized by a wet chemical method and their phosphate adsorption characteristics & mechanism. Ceramics International, 2022, 48: 6591-6599

4. Lin J, Zhan Y, Wang H, Chu M, Wang C, He Y, Wang X. Effect of calcium ion on phosphate adsorption onto hydrous zirconium oxide. Chemical Engineering Journal, 2017, 309: 118-129
5. Zong E, Liu X, Jiang J, Fu S, Chu F. Preparation and characterization of zirconia-loaded lignocellulosic butanol residue as a biosorbent for phosphate removal from aqueous solution. Applied Surface Science, 2016, 387: 419-430
6. Bui T H, Hong S P, Kim C, Yoon J. Performance analysis of hydrated Zr(IV) oxide nanoparticle-impregnated anion exchange resin for selective phosphate removal. Journal of Colloid and Interface Science, 2021, 586: 741-747
7. Zhao Y, Shan X, An Q, Xiao Z, Zhai S. Interfacial integration of zirconium components with amino-modified lignin for selective and efficient phosphate capture. Chemical Engineering Journal, 2020, 398: 125561